EMBO reports

EMBO open

scientific report

Five dysfunctional telomeres predict onset of senescence in human cells

Zeenia Kaul[1,2], Anthony J. Cesare[1,2†], Lily I. Huschtscha[1,2], Axel A. Neumann[1,2] & Roger R. Reddel[1,2+]

[1]Cancer Research Unit, Children's Medical Research Institute, Westmead, and [2]Sydney Medical School, University of Sydney, Sydney, New South Wales, Australia

Replicative senescence is accompanied by a telomere-specific DNA damage response (DDR). We found that DDR+ telomeres occur spontaneously in early-passage normal human cells and increase in number with increasing cumulative cell divisions. DDR+ telomeres at replicative senescence retain TRF2 and RAP1 proteins, are not associated with end-to-end fusions and mostly result from strand-independent, postreplicative dysfunction. On the basis of the calculated number of DDR+ telomeres in G1-phase cells just before senescence and after bypassing senescence by inactivation of wild-type p53 function, we conclude that the accrual of five telomeres in G1 that are DDR+ but nonfusogenic is associated with p53-dependent senescence.

Keywords: telomeres; DNA damage response; senescence

EMBO *reports* (2012) **13**, 52–59. doi:10.1038/embor.2011.227

INTRODUCTION

Normal human cells divide a limited number of times before entering an irreversible cell cycle arrest termed replicative senescence (Hayflick & Moorhead, 1961). Telomeres shorten in human somatic cells with each cell division, and it has been suggested that they function as a replicometer determining the onset of senescence (Harley *et al*, 1990). Expression of some oncogenes can bypass senescence and confer a finite life span extension that eventually ends in culture crisis. Rarely, cells escape crisis and become immortalized (Girardi *et al*, 1965) by activating a telomere maintenance mechanism to offset telomere erosion (Colgin & Reddel, 1999).

Human telomeres contain 4–12 kb of 5′-TTAGGG-3′ repeats ending in a single-stranded overhang of the G-rich sequence, and are bound extensively by the six-subunit shelterin protein complex (Palm & de Lange, 2008). Telomeres can adopt a loop (t-loop) structure (Griffith *et al*, 1999). Telomere length-independent deprotection of telomeres via disruption of shelterin proteins induces p53-dependent senescence (van Steensel *et al*, 1998; Hockemeyer *et al*, 2005; Guo *et al*, 2007). Under these conditions, DNA damage response (DDR) factors such as phosphorylated H2AX (γ-H2AX) and 53BP1 colocalize with telomeres in telomere dysfunction-induced foci (TIFs; Takai *et al*, 2003). Similar foci occur in smaller numbers at replicative senescence and there is evidence that these telomeric DDR signals are responsible for initiating p53-dependent senescence (d'Adda di Fagagna *et al*, 2003).

We have previously proposed a three-state model of telomere end protection (Cesare *et al*, 2009). In this model, the 'closed state' is a telomere length-dependent structure that protects chromosome ends against a DDR. Although the closed-state conformation is unknown, a t-loop fulfils the predicted requirements of being a shelterin-mediated, length-dependent protective structure. The 'intermediate state' is proposed to be partly protective: the telomere induces a DDR, but binds sufficient shelterin to inhibit end-to-end fusion. The 'uncapped state' is both DDR+ and fusogenic and might result from a level of shelterin binding that is insufficient to prevent end-to-end fusions.

It has been proposed previously that a single unrepaired double-strand break in human cells is sufficient to arrest cell growth (Di Leonardo *et al*, 1994), but the quantitative relationship between DDR+ telomeres and growth arrest needed to be established. We also aimed at determining whether DDR+ telomeres at senescence are in an intermediate or uncapped state, and whether they occur predominantly after leading- or lagging-strand synthesis. We therefore examined the quantitative relationship between spontaneous telomere dysfunction and the *in vitro* proliferative life span of normal human cells.

RESULTS

Spontaneous telomere dysfunction increases as cells age

We obtained normal diploid skin fibroblasts (Fre 71s-1, 74s-1a, 92s-2 and 102s-3), stromal fibroblasts (Fre 80) and epithelial cells (Bre 102–170; same donor as Fre 102s-3) from the breast tissue of five healthy human donors (Fig 1A,B). The epithelial culture grew for three population doublings (PDs) before cell numbers reached

[1]Cancer Research Unit, Children's Medical Research Institute, 214 Hawkesbury Road, Westmead, New South Wales 2145, Australia
[2]Sydney Medical School, University of Sydney, Sydney, New South Wales 2006, Australia
[†]Present address: Molecular and Cellular Biology Department, The Salk Institute for Biological Studies, 10010 North Torrey Pines Road, La Jolla, California 92037-1099, USA
[+]Corresponding author. Tel: + 612 8865 2901; Fax: + 612 8865 2860;
E-mail: rreddel@cmri.org.au

Received 13 June 2011; revised 11 October 2011; accepted 25 October 2011; published online 9 December 2011

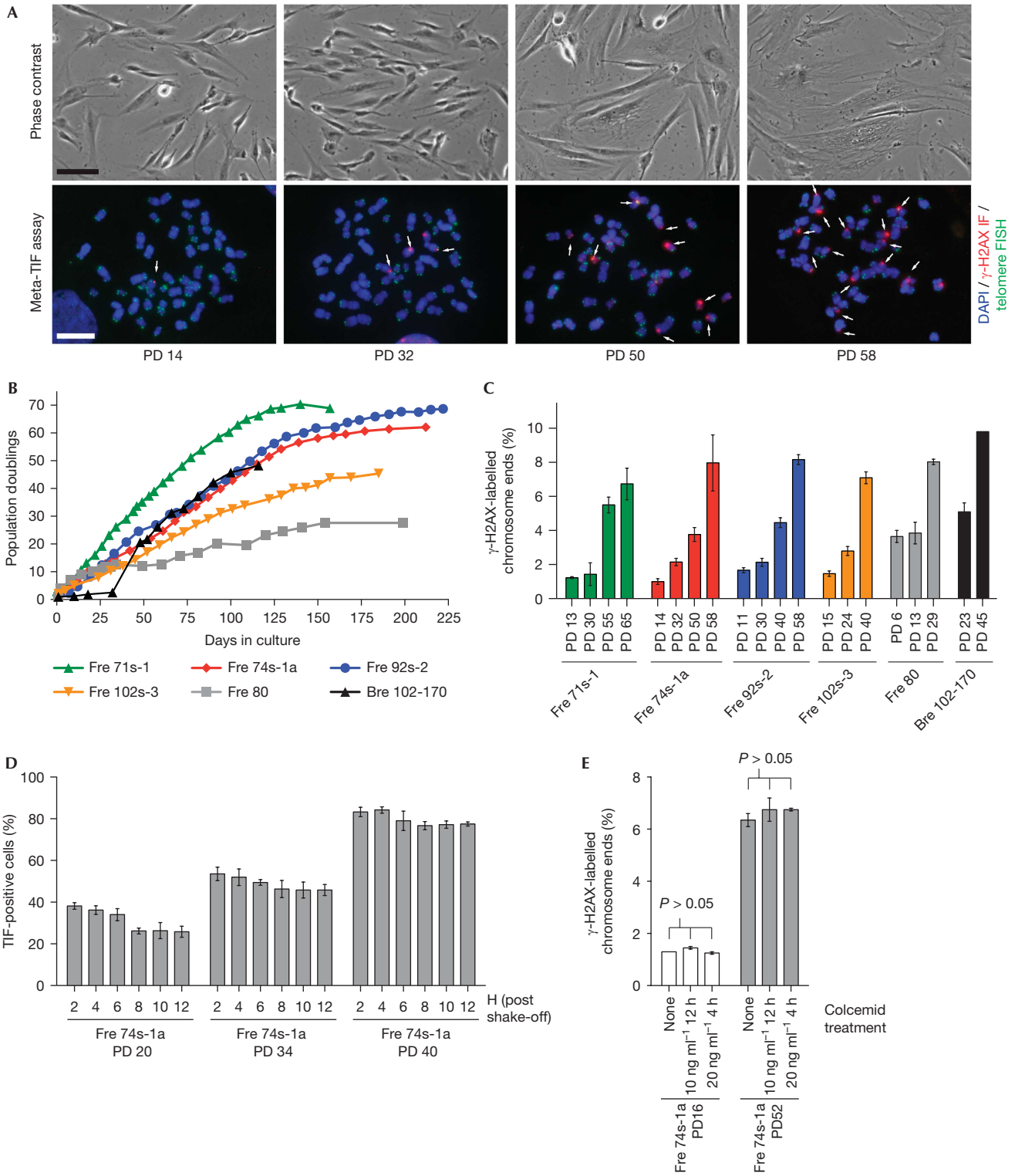

Fig 1 | Spontaneous telomere dysfunction in normal human cells. (**A**) Phase-contrast microscopy and meta-TIF assay images of Fre 74s-1 cells. Meta-TIF assay samples were stained with DAPI (blue), γ-H2AX IF (red) and telomere FISH (green). White arrows: meta-TIFs; black bars: 50 μm; white bars: 10 μm. (**B**) Growth curves. (**C**) Meta-TIF assay results (mean ± s.d., $n = 3$). (**D**) Percentage of γ-H2AX TIF-positive nuclei after treatment with 20 ng ml^{-1} colcemid for 4 h, mitotic shake-off, plating and fixation at indicated times (mean ± s.d., $n = 3$ experiments quantifying 100 nuclei). (**E**) Meta-TIF assay results after indicated colcemid treatments (average ± range, $n = 2$; *P*, Student *t*-test). DAPI, 4′,6-diamidino-2-phenylindole; FISH, fluorescence *in situ* hybridization; γ-H2AX, phosphorylated H2AX; IF, immunofluorescence; meta-TIF, metaphase telomere dysfunction-induced focus; PD, population doubling.

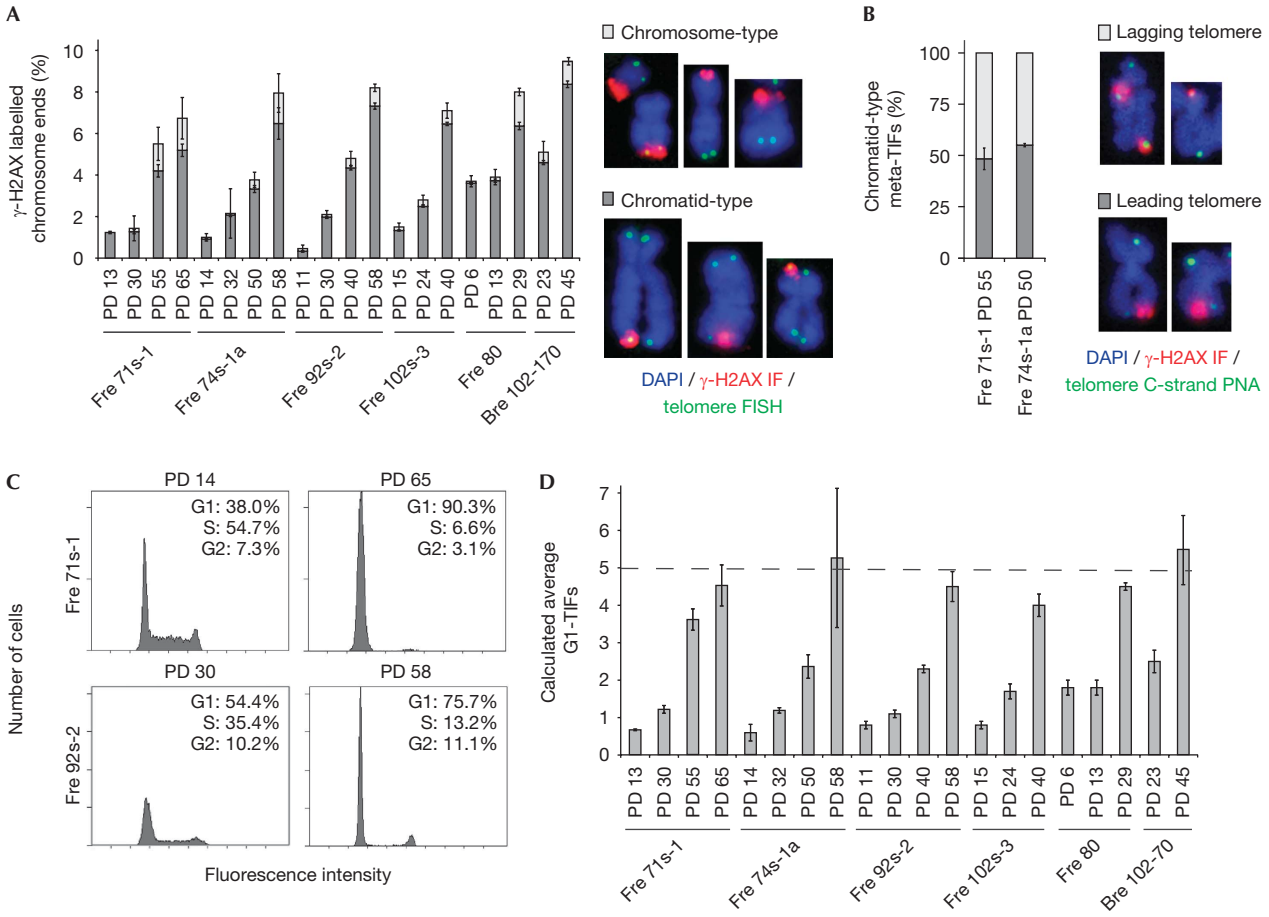

Fig 2 | Five DDR+ telomeres precede replicative senescence. (**A**) Chromosome- and chromatid-type meta-TIFs as a percentage of total meta-TIFs (mean ± s.d., $n = 3$). Examples of chromatid- and chromosome-type meta-TIFs stained with DAPI (blue), γ-H2AX IF (red) and telomere FISH (green). (**B**) CO-meta-TIF assay results (mean ± s.d., $n = 3$) and examples stained with DAPI (blue), γ-H2AX IF (red) and telomere C-strand PNA FISH (green). (**C**) Flow cytometry of PI-stained dividing and senescent normal fibroblasts. (**D**) Calculated number of predicted G1-TIFs. CO, chromosome orientation; DAPI, 4′,6-diamidino-2-phenylindole; DDR, DNA damage response; FISH, fluorescence *in situ* hybridization; γ-H2AX, phosphorylated H2AX; IF, immunofluorescence; meta-TIF, metaphase telomere dysfunction-induced focus; PD, population doubling; PI, propidium iodide; PNA, peptide nucleic acid.

a plateau and a subpopulation of cells emerged and proliferated until PD 45, consistent with previous observations (Stampfer, 1985; Huschtscha *et al*, 1998). Late-PD cultures exhibited markers of replicative senescence, including altered cell morphology (Fig 1A), increased numbers of β-galactosidase-positive cells, increased p21 protein levels and progressive telomere shortening (supplementary Fig S1 online).

We showed previously that spontaneous telomere dysfunction can be quantified by detecting metaphase TIFs (meta-TIFs) in cytocentrifuged metaphase spreads stained by immunofluorescence (IF) against γ-H2AX and telomere fluorescent *in situ* hybridization (FISH; Cesare *et al*, 2009). We analysed meta-TIFs at multiple times during the growth of each culture, scoring chromosome ends labelled with γ-H2AX IF at one or both sister chromatids, with and without a detectable telomere FISH signal. Meta-TIFs increased with increasing PDs but, surprisingly, all cultures had DDR+ telomeres (Fig 1A,C). To exclude the possibility that meta-TIFs in ageing cells are a transient mitotic phenomenon, mitotic cells were collected from asynchronous cultures by shake-off, plated on coverslips and fixed at 2-h intervals, and interphase TIFs were detected by γ-H2AX IF and telomere FISH. Interphase nuclei with one or more γ-H2AX-positive telomeres were observed at all PDs tested, with the percentage of TIF+ cells increasing with increasing PDs (Fig 1D). TIF+ cells persisted for 12 h after shake-off. We therefore conclude that TIFs are passed from mitosis into the G1 cell cycle phase, and that normal human cells tolerate a small number of DDR+ telomeres without ceasing proliferation. We showed that spontaneous meta-TIFs are not an artefact of the very low doses of colcemid (10 or 20 ng ml^{-1}) used for this assay (Fig 1E).

Characterization of spontaneous telomere dysfunction

We refer to meta-TIFs with γ-H2AX staining on one or both sister chromatids as 'chromatid type' and 'chromosome type', respectively (Fig 2A). Chromatid-type meta-TIFs most probably arise because of replicative or postreplicative dysfunction affecting one

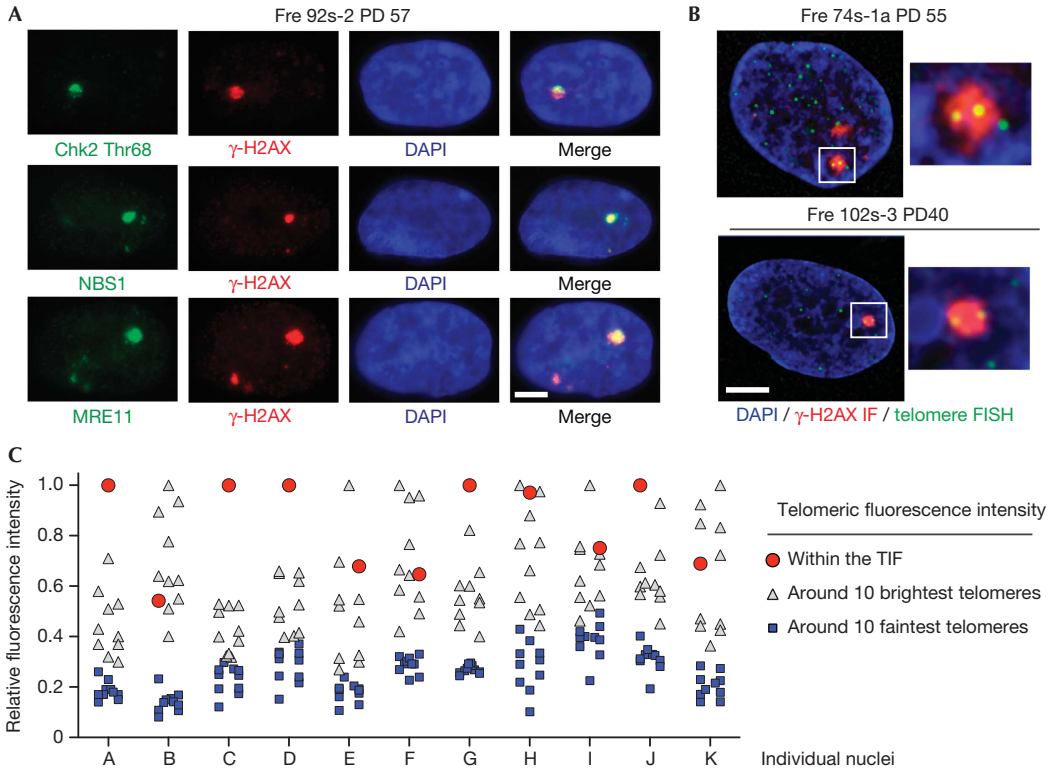

Fig 3 | TIFs aggregate in senescent nuclei. (**A**) Senescent nuclei stained with DAPI (blue), γ-H2AX IF (red) and Chk2-Thr68, NBS1 or MRE11 IF (green). (**B**) Senescent nuclei stained with DAPI (blue), γ-H2AX IF (red) and telomere FISH (green). Images shown are a single deconvolved focal plane. Enlargements are shown at the right. White bars in (**A**) and (**B**): 5 μm. (**C**) Relative telomeric fluorescence intensity in 11 Fre 102s-3 nuclei within a circle drawn around the boundaries of a γ-H2AX focus (red circle) and the same circle around each of the 10 brightest (grey triangles) and 10 faintest (blue squares) telomeres in the same nuclei. DAPI, 4′,6-diamidino-2-phenylindole; FISH, fluorescence *in situ* hybridization; γ-H2AX, phosphorylated H2AX; IF, immunofluorescence; TIF, telomere dysfunction-induced focus.

sister-chromatid telomere (Cesare *et al*, 2009). In every culture, meta-TIFs were predominantly chromatid-type (Fig 2A), indicating that telomere dysfunction in aged human cells mostly results from events during or after replication.

The C- and G-rich telomeric DNA strand is always the leading- and lagging-strand replication template, respectively, and induced telomere dysfunction was previously observed to be strand specific in human cells (Bailey *et al*, 2001; Crabbe *et al*, 2004; Deng *et al*, 2009; Dimitrova & de Lange, 2009). Combining telomere chromosome orientation (CO)-FISH (Bailey *et al*, 2001) and the meta-TIF assay (Cesare *et al*, 2009) identifies leading- or lagging-strand-derived chromatid-type meta-TIFs (supplementary Fig S2 online). For two late-PD fibroblast cultures, CO-meta-TIF analysis showed that 48.4 ± 5.3% and 55.1 ± 0.8% of chromatid-type meta-TIFs were on the leading telomere in Fre71s-1 and Fre74s-1a cells, respectively (Fig 2B), indicating that spontaneous postreplicative telomere dysfunction in aged normal fibroblasts is unlikely to be strand specific.

Five dysfunctional telomeres precede senescence

Our observation that small numbers of TIFs are present in dividing presenescent cultures suggests that a threshold number of dysfunctional telomeres is required to induce senescence. Flow cytometry showed that most senescent cells were arrested in G1 (Fig 2C), suggesting that the number of TIFs in G1 is probably responsible for senescence induction. We expect segregation of chromatid- or chromosome-type meta-TIFs to result in one or both daughter cells, respectively, inheriting a TIF (supplementary Fig S3A online). By assuming random segregation of chromatid-type meta-TIFs, we calculated the average number of G1-TIFs and found that senescent G1-phase nuclei would contain four or five TIFs (Fig 2D; supplementary Fig S3B–D online).

Dysfunctional telomeres aggregate

Earlier studies have identified typically one or two spontaneous TIFs in senescent interphase nuclei (Zou *et al*, 2004), which seems inconsistent with our calculation of 4–5 G1-TIFs per senescent cell. When we stained interphase senescent cells, we also commonly found one or two large γ-H2AX foci per nucleus that colocalized with the DDR proteins MRE11 and NBS1 (Fig 3A). However, deconvolved images showed that 71.2 ± 1.3% of senescent nuclei (mean ± s.d., $n = 3$ experiments, each examining 25 nuclei) had multiple telomeres colocalized within individual γ-H2AX foci, suggesting that dysfunctional telomeres aggregate in senescent cells (Fig 3B). To test this further, we measured the mean telomeric fluorescence intensity in γ-H2AX foci of 11 senescent nuclei and compared this with that of the 10 brightest and 10 faintest telomere signals in the same nuclei. The telomeric

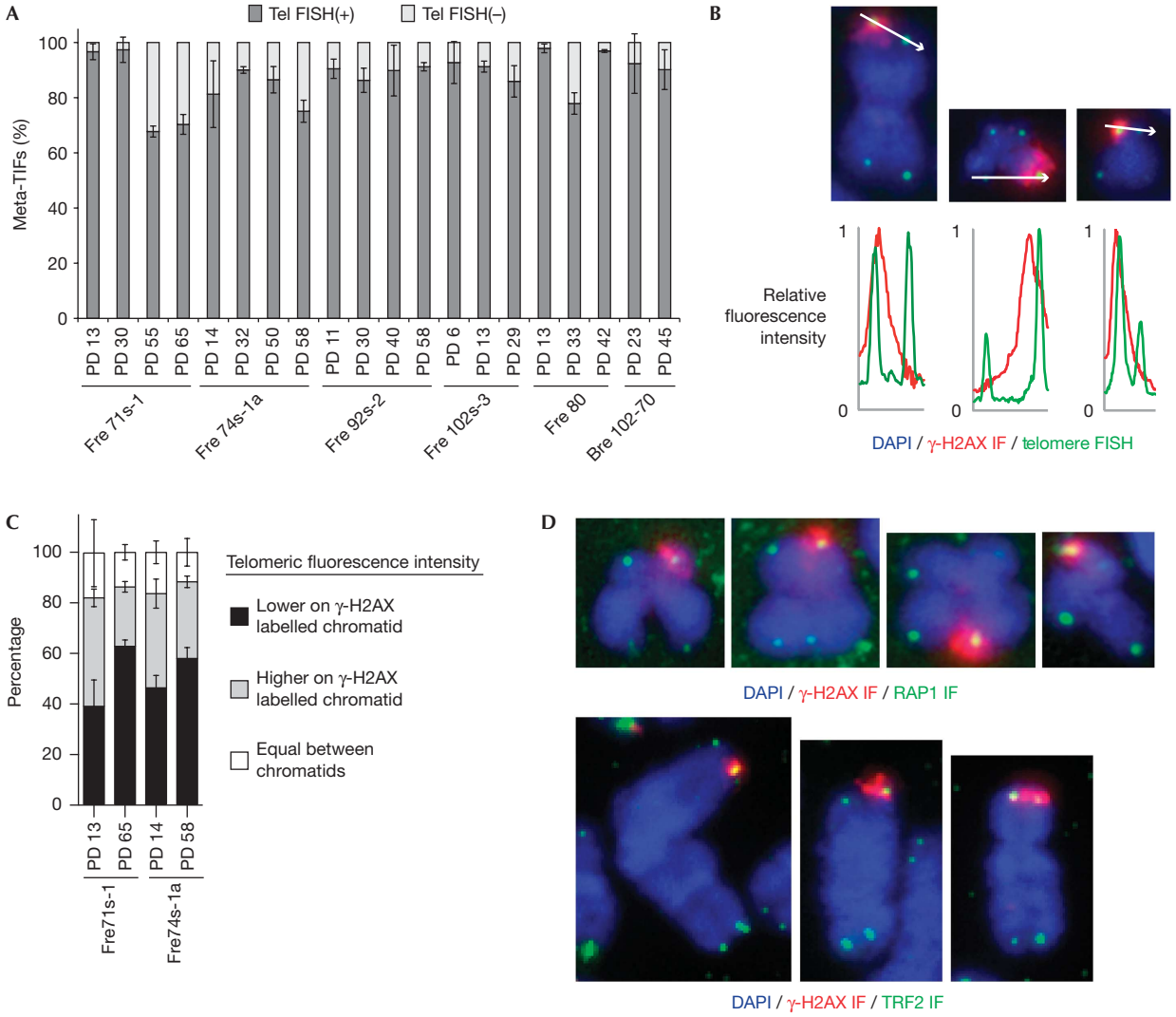

Fig 4 | Relationship between telomere length and meta-TIFs. (**A**) Percentage of meta-TIFs with detectable (+) or undetectable (−) telomere FISH signals (mean ± s.d., $n = 3$). (**B**) Comparison of relative fluorescence intensity of γ-H2AX IF (red) and telomere FISH (green). (**C**) Quantification of relative telomeric fluorescence intensity between the γ-H2AX-positive and -negative sister telomeres of a chromosome-type meta-TIF (mean ± s.d., $n = 3$). (**D**) Cyto-centrifuged chromosomes stained with DAPI (blue), γ-H2AX IF (red) and TRF2 or RAP1 IF (green). DAPI, 4′,6-diamidino-2-phenylindole; DDR, DNA damage response; FISH, fluorescence *in situ* hybridization; γ-H2AX, phosphorylated H2AX; IF, immunofluorescence; meta-TIF, metaphase telomere dysfunction-induced focus; PD, population doubling; Tel, telomere.

signal within the γ-H2AX focus was always brighter than the faintest telomeres and often brighter than the brightest individual telomeres within the cell, consistent with the conclusion that a single γ-H2AX focus might contain aggregates of dysfunctional telomeres (Fig 3C).

Dissociation of telomere length and dysfunction

Although meta-TIF numbers increased with increasing PDs and thus with decreasing telomere length, analysis of individual telomeres showed that telomere length and DDR were sometimes dissociated. Most meta-TIFs had detectable telomere FISH signals, even at the PD immediately preceding senescence, indicating that the DDR did not result from lack of telomeric DNA (Fig 4A). Examination of telomere FISH signal intensity at chromatid-type meta-TIFs showed that although the γ-H2AX+ chromatid usually had a lower telomere FISH signal intensity than its γ-H2AX− sister, the converse also occurred (Fig 4B,C). In addition, we observed RAP1 and TRF2 staining at γ-H2AX+ chromosome ends, indicating that these shelterin proteins are retained at spontaneously dysfunctional telomeres in aged human cells (Fig 4D).

Telomere dysfunction during lifespan extension

Numerous studies have shown that p53 is involved in cellular senescence and that the ability of simian virus 40 to extend the proliferative life span is dependent on its large T-antigen (LT) protein inactivating p53 and Rb; the period of extended life span for LT-expressing cells ends in crisis (Bryan & Reddel, 1994).

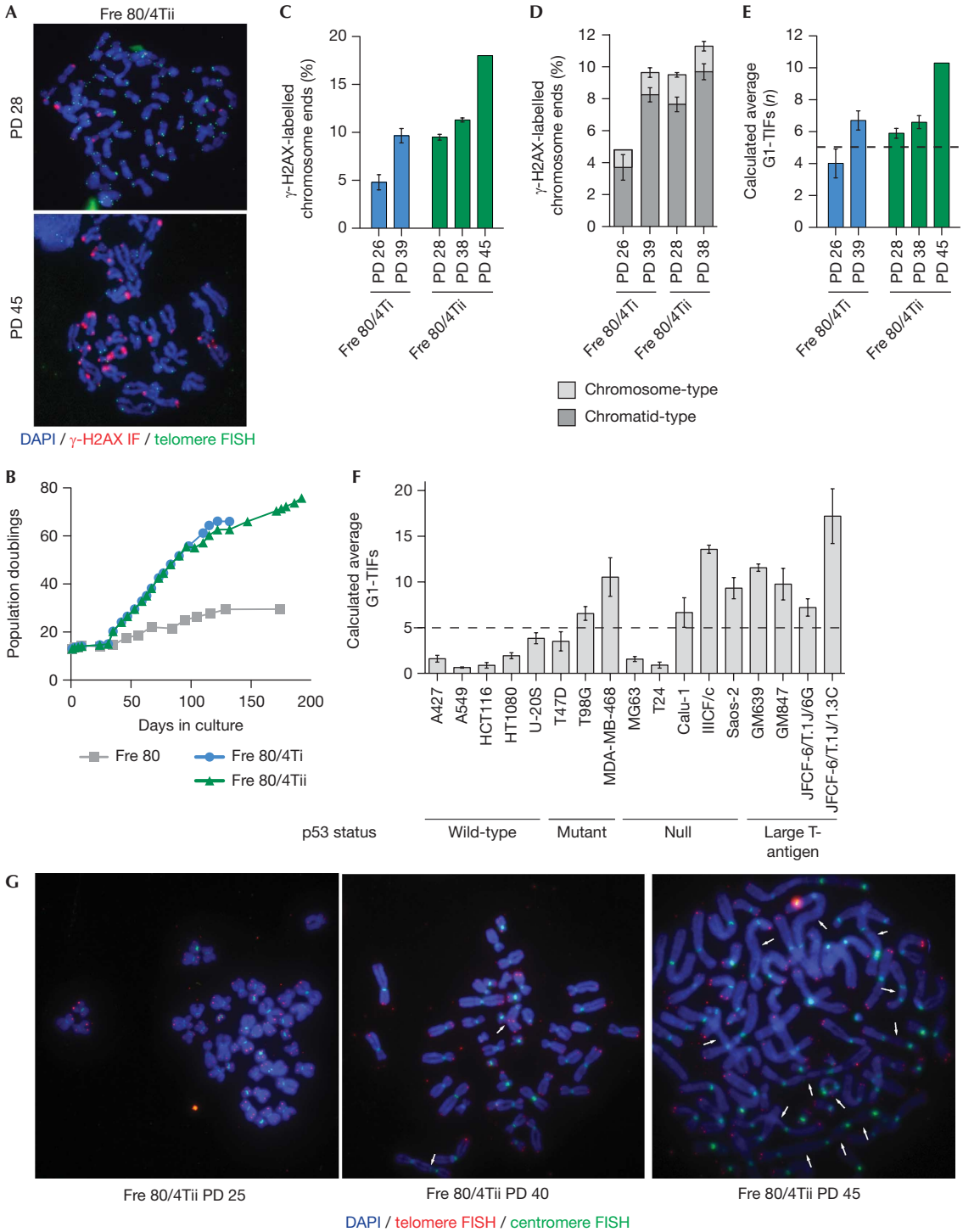

Fig 5 | Telomere dysfunction during lifespan extension and crisis. (**A**) Meta-TIF assay images from simian virus 40 LT-transfected cells (Fre 80/4Tii) at PD 28 and 45. (**B**) Growth curves. (**C**) Meta-TIF assays (average ± range, $n = 2$; except for Fre 80/4Tii PD 45, $n = 1$). (**D**) Contribution of chromosome- and chromatid-type meta-TIFs (average ± range, $n = 2$). (**E**) Calculated number of G1-TIFs. (**F**) Calculated number of G1-TIFs from meta-TIF data for 17 immortalized cell lines (Cesare *et al*, 2009). (**G**) Representative images of standard cytogenetic preparations from Fre 80 and Fre 80/4Tii stained with telomere (red) and centromere (green) FISH; examples of fused chromosomes are indicated by white arrows. DAPI, 4′,6-diamidino-2-phenylindole; FISH, fluorescence *in situ* hybridization; LT, large T-antigen; meta-TIF, metaphase telomere dysfunction-induced focus; PD, population doubling.

We generated two cultures, Fre 80/4Ti and Fre 80/4Tii, by transfecting Fre 80 cells with LT to test the hypothesis that loss of p53 function allows cells to bypass cell cycle arrest in the presence of more than five G1-TIFs per cell. As expected, there was LT expression but no telomerase activity during the lifespan extension period (supplementary Fig S4A,B online). Meta-TIFs increased during lifespan extension, and were predominantly chromatid-type; in crisis cells, different meta-TIF types were unable to be distinguished for technical reasons (Fig 5A–D). We calculated that there was an average of more than five G1-TIFs per cell during lifespan extension (Fig 5E; supplementary Fig 4C online).

To further test our hypothesis, we mined data from a previous study investigating spontaneous meta-TIFs in immortalized cells (Cesare *et al*, 2009). The predicted content of G1-TIFs was on average less than five per cell in all cell lines with wild-type p53 function, and was typically more than five per cell in cell lines lacking p53 transactivation activity (Fig 5F). This is consistent with the conclusion that five dysfunctional telomeres in G1 are sufficient to induce p53-dependent cell cycle arrest.

In untransfected normal cells, chromosome fusions were not observed in any metaphase, including the one at the PD immediately preceding replicative senescence. We counted end-to-end chromosome fusions in metaphases prepared by standard cytogenetic methods from Fre 80 and Fre 80/4Tii cells and observed fusions only in cells that had bypassed senescence (Fig 5G; supplementary Fig 4D online).

DISCUSSION

We found that meta-TIFs were present in early-passage cultures of normal human cells and increased in number until senescence, when the calculated number of TIFs in G1-phase cells was approximately five. In cells that bypassed senescence temporarily because of abrogation of wild-type p53 function, and in p53-deficient immortalized cells, the calculated number of G1-TIFs exceeded five. The most likely interpretation is that replicative senescence is initiated in a p53-dependent manner when the integrated signalling from DDR+ telomeres reaches a threshold level, but formal proof will require the development of an experimental system to induce limited numbers of non-fusogenic, DDR+ telomeres in human cells. We cannot exclude the possibility, for example, that only a fully deprotected telomere can initiate senescence, and that the probability of this occurring becomes very high when the number of G1-TIFs has reached five. Nevertheless, our results clearly indicate that normal human cells are able to tolerate small numbers of DDR+ telomeres.

Several factors might contribute to the difference between the calculated numbers of G1-phase DDR+ telomeres in low-PD cells and previously published data indicating somewhat lower numbers of interphase TIFs in young cells (d'Adda di Fagagna *et al*, 2003; Herbig *et al*, 2004). First, interphase counts in other studies include cells in phases other than G1. Second, our data indicate that it is likely that some DDR+ telomeres are repackaged in early G1 and become DDR−. Third, we consistently observe that meta-TIFs are brighter and easier to detect than interphase-TIFs (data not shown), possibly because of differences in epitope presentation on mitotic chromatin. Finally, the aggregation of DDR+ telomeres we observed in interphase TIFs would result in lower counts. The latter observation is also of interest because aggregation of DDR foci at breaks elsewhere in the genome poses the risk of inappropriate repair reactions, but presumably this is not problematic in the case of DDR+ telomeres that are able to suppress end-to-end fusions.

The observed characteristics of DDR+ telomeres at senescence are consistent with those of the putative 'intermediate state' in our three-state telomere model (Cesare *et al*, 2009). We observed end-to-end fusions in cells that bypassed senescence, presumably due to extreme telomere shortening and loss of shelterin-binding capacity, and accounting for the extensive cell death characteristic of crisis, but not in any pre-senescent cells, presumably because their DDR+ telomeres retain sufficient binding of shelterin proteins including TRF2 and RAP1. Moreover, most of the pre-senescent DDR foci occurred only on one sister chromatid, suggesting that they resulted from a post-replicative event. Although the number of TIFs correlated inversely with telomere length, in some cases the DDR+ sister chromatid had more telomeric DNA than its protected sister. This supports previous conclusions that telomere structure, rather than telomere length *per se*, regulates senescence induction (Karlseder *et al*, 2002). We suggest that failure to form a closed state during S or G2 phase results in intermediate-state telomeres persisting into M and G1 phases. Some intermediate-state telomeres are probably repackaged into closed-state structures during G1, as we observed a slight reduction in the number of TIF+ G1 cells until ~8 h after mitotic shake-off.

It has been proposed that telomere structure is reset in each cell cycle after DNA replication (Verdun & Karlseder, 2007), and a corollary of this might be that an intermediate-state telomere formed during one cell cycle can adopt a closed state in the following cell cycle, provided the telomere retains sufficient telomere length and thus sufficient shelterin-binding capacity. In this view, formation of an intermediate-state telomere is a stochastic event, with the probability of its occurrence increasing with decreasing telomere length. Although some chromosome-type meta-TIFs might simply represent the chance occurrence of intermediate-state telomeres on both sister chromatids, some might represent telomeres that have shortened below the absolute length required to form a fully protective structure, so that the probability of forming an intermediate-state telomere is now 100%.

The absence of end-to-end fusions in replicative senescence, in contrast to the rampant fusions, genomic instability and cell death in crisis, suggests that telomere structure provides an elegant mechanism for limiting the normal replicative life span without excessive risk of genomic instability. With increasing PDs, the fully protective closed-state telomere structure (possibly involving a t-loop) progressively fails to form, resulting in a structure that contributes to the integrated signal initiating onset of senescence while still protecting against fusion events.

METHODS

Cell culture and transfection. Primary cultures were obtained from tissue donated with informed consent by individuals undergoing elective reduction mammoplasties and with human ethics committee approval. Epithelial cells were grown in serum-free MCDM-170 medium (Gibco) and fibroblasts were grown in Dulbecco's modified Eagle's medium plus 10% (v/v) fetal bovine serum. All cultures were mycoplasma free and grown without antibiotics in a humidified incubator at 37 °C with 5% CO_2.

Cells were transfected with a plasmid (pRSV-T) encoding the simian virus 40 early region using Fugene-6 (Roche).

Antibodies. The primary antibodies used were γ-H2AX (613402, BioLegend, or IHC-00059-1, Bethyl Laboratories), MRE11 (100-142 G2, Novus Biologicals), NBS1 (611871, BD Transduction), Chk2-Thr 68 (2661S, Cell Signaling Technologies), TRF2 (110-57130, Novus Biologicals) and RAP1 (NS100-292, Novus Biologicals). Fluorophore-conjugated secondary antibodies used were A11034 and A11032 (Invitrogen).

Mitotic shake-off. Cells were treated with 20 ng ml^{-1} colcemid for 4 h and mitotic cells were detached into the medium by tapping the flask. Cells were collected by centrifugation and plated on sterile glass coverslips, and then fixed in 4% formaldehyde at 2, 4, 6, 8, 10 or 12 h before γ-H2AX IF and telomere FISH.

Meta-TIF and CO-meta-TIF assays. Early and late PD cultures were treated with 20 ng ml^{-1} colcemid (Gibco) for 1–4 h and 10 ng ml^{-1} colcemid for 8–12 h, respectively. All other steps were performed as described (Cesare *et al*, 2009) and 25 metaphases were quantified per replicate. The supplementary information online contains the details of the G1-TIF calculations.

Chromosome fusion analysis. Chromosome preparations were obtained according to standard cytogenetic methods and hybridized with a Texas Red-conjugated telomere PNA probe and fluorescein isothiocyanate-conjugated centromere PNA probe (5′-AAACACTCTTTTTGTAGA-3′; Applied Biosystems).

Immunostaining and telomere FISH on interphase nuclei. Cells grown on sterile glass coverslips were fixed with 100% methanol or 1 × PBS + 4% (v/v) formaldehyde. For MRE11 staining, cells were pre-extracted using 20 mM HEPES, 50 mM NaCl, 3 mM $MgCl_2$, 300 mM sucrose and 0.5% Triton X-100 (v/v) before fixation. IF and/or telomere FISH was performed as described (Cesare *et al*, 2009).

Imaging. Imaging was performed as described (Cesare *et al*, 2009). Fluorescent intensity was determined using the ImagePro Plus software (version 4.5.1, Media Cybernetics Inc.).

Cell cycle analysis. Cells were collected at approximately 60% confluence, fixed with ice-cold 80% (v/v) ethanol for 30 min, washed twice with 1 × PBS + 0.1% (w/v) EDTA and collected by centrifugation. Cells were resuspended in 0.03 mg ml^{-1} propidium iodide (Sigma) and 0.3 mg ml^{-1} RNAse A (Sigma), incubated at 37 °C for 30 min and then at room temperature overnight. DNA content was analysed using a Beckman Coulter FACS FC 500.

Supplementary information is available at EMBO *reports* online (http://www.emboreports.org).

ACKNOWLEDGEMENTS

We thank Dr Daniel Speidel for experimental assistance and Dr Makoto Hayashi and Dr Jan Karlseder for sharing unpublished data. This work was supported by an Australian Postgraduate Award, a Judith Hyam Memorial Trust Fund for Cancer Research Scholarship and a Research Scholar Award from Cancer Institute NSW (to Z.K.); a USA National Science Foundation International Research Fellowship (0602009) and a project grant from Cure Cancer Australia Foundation (to A.J.C.); and a Cancer Council NSW Program Grant (to R.R.R.).

Author contributions: Z.K., A.J.C., L.I.H. and A.A.N. performed the experiments. Z.K., A.J.C. and R.R.R. conceived the study, performed data analysis and wrote the manuscript.

CONFLICT OF INTEREST

The authors declare that they have no conflict of interest.

REFERENCES

Bailey SM, Cornforth MN, Kurimasa A, Chen DJ, Goodwin EH (2001) Strand-specific postreplicative processing of mammalian telomeres. *Science* **293:** 2462–2465

Bryan TM, Reddel RR (1994) SV40-induced immortalization of human cells. *Crit Rev Oncog* **5:** 331–357

Cesare AJ, Kaul Z, Cohen SB, Napier CE, Pickett HA, Neumann AA, Reddel RR (2009) Spontaneous occurrence of telomeric DNA damage response in the absence of chromosome fusions. *Nat Struct Mol Biol* **16:** 1244–1251

Colgin LM, Reddel RR (1999) Telomere maintenance mechanisms and cellular immortalization. *Curr Opin Genet Dev* **9:** 97–103

Crabbe L, Verdun RE, Haggblom CI, Karlseder J (2004) Defective telomere lagging strand synthesis in cells lacking WRN helicase activity. *Science* **306:** 1951–1953

d'Adda di Fagagna F, Reaper PM, Clay-Farrace L, Fiegler H, Carr P, von Zglinicki T, Saretzki G, Carter NP, Jackson SP (2003) A DNA damage checkpoint response in telomere-initiated senescence. *Nature* **426:** 194–198

Deng Y, Guo X, Ferguson DO, Chang S (2009) Multiple roles for MRE11 at uncapped telomeres. *Nature* **460:** 914–919

Di Leonardo A, Linke SP, Clarkin K, Wahl GM (1994) DNA damage triggers a prolonged p53-dependent G1 arrest and long-term induction of Cip1 in normal human fibroblasts. *Genes Dev* **8:** 2540–2551

Dimitrova N, de Lange T (2009) Cell cycle dependent role of MRN at dysfunctional telomeres: ATM signaling-dependent induction of nonhomologous end joining (NHEJ) in G1 and resection-mediated inhibition of NHEJ in G2. *Mol Cell Biol* **29:** 5552–5563

Girardi AJ, Jensen FC, Koprowski H (1965) SV40-induced transformation of human diploid cells: crisis and recovery. *J Cell Comp Physiol* **65:** 69–84

Griffith JD, Comeau L, Rosenfield S, Stansel RM, Bianchi A, Moss H, de Lange T (1999) Mammalian telomeres end in a large duplex loop. *Cell* **97:** 503–514

Guo X, Deng Y, Lin Y, Cosme-Blanco W, Chan S, He H, Yuan G, Brown EJ, Chang S (2007) Dysfunctional telomeres activate an ATM-ATR-dependent DNA damage response to suppress tumorigenesis. *EMBO J* **26:** 4709–4719

Harley CB, Futcher AB, Greider CW (1990) Telomeres shorten during ageing of human fibroblasts. *Nature* **345:** 458–460

Hayflick L, Moorhead PS (1961) The serial cultivation of human diploid cell strains. *Exp Cell Res* **25:** 585–621

Herbig U, Jobling WA, Chen BP, Chen DJ, Sedivy JM (2004) Telomere shortening triggers senescence of human cells through a pathway involving ATM, p53, and p21(CIP1), but not p16INK4A. *Mol Cell* **14:** 501–513

Hockemeyer D, Sfeir AJ, Shay JW, Wright WE, de Lange T (2005) POT1 protects telomeres from a transient DNA damage response and determines how human chromosomes end. *EMBO J* **24:** 2667–2678

Huschtscha LI, Noble JR, Neumann AA, Moy EL, Barry P, Melki JR, Clark SJ, Reddel RR (1998) Loss of $p16^{INK4}$ expression by methylation is associated with lifespan extension of human mammary epithelial cells. *Cancer Res* **58:** 3508–3512

Karlseder J, Smogorzewska A, de Lange T (2002) Senescence induced by altered telomere state, not telomere loss. *Science* **295:** 2446–2449

Palm W, de Lange T (2008) How shelterin protects mammalian telomeres. *Annu Rev Genet* **42:** 301–334

Stampfer MR (1985) Isolation and growth of human mammary epithelial cells. *J Tissue Cult Methods* **9:** 107–115

Takai H, Smogorzewska A, de Lange T (2003) DNA damage foci at dysfunctional telomeres. *Curr Biol* **13:** 1549–1556

van Steensel B, Smogorzewska A, de Lange T (1998) TRF2 protects human telomeres from end-to-end fusions. *Cell* **92:** 401–413

Verdun RE, Karlseder J (2007) Replication and protection of telomeres. *Nature* **447:** 924–931

Zou Y, Sfeir A, Shay JW, Wright WE (2004) Does a sentinel or a subset of short telomeres determine replicative senescence? *Mol Biol Cell* **15:** 3709–3718